GRIDLESS ANGLE AND RANGE ESTIMATION FOR FDA-MIMO RADAR BASED ON DECOUPLED ATOMIC NORM MINIMIZATION

Wen-Gen Tang, Hong Jiang, Shuai-Xuan Pang

College of Communication Engineering, Jilin University, Changchun, 130012, China

ABSTRACT

The frequency diverse array (FDA), which exploits a small frequency increment across the transmitting antenna elements, has been recently introduced to multiple-input-multiple-output (MIMO) radar to offer the capability of range-angle-dependent beampattern and target localization. Traditionally, the two-dimensional (2D) subspace-based methods and grid-based sparse reconstruction algorithms are used to obtain angle and range in FDA-MIMO radar. In this paper, with a single measurement, we propose a gridless angle and range estimation approach for FDA-MIMO radar based on decoupled atomic norm minimization (DANM). First, we convert the 2D-ANM based angle and range estimation into a decoupled semi-definite programming problem with two one-dimensional (1D) Toeplitz Hermitian matrices. Then we apply the matrix enhancement and matrix pencil method and construct a permutation matrix to obtain joint angle and range estimation and parameter pairing. Numerical results verify that the proposed approach overcomes the grid-mismatch effect of the sparse reconstruction-based OMP algorithm and outperforms the subspace-based MUSIC method.

Index Terms— Frequency diverse array, multiple-input-multiple-output radar, angle and range estimation, atomic norm minimization, gridless parameter estimation

1. INTRODUCTION

Multiple-input-multiple-output (MIMO) radar is attractive for efficiently exploiting the spatial diversity and high number of degrees of freedom (DOF) to improve resolution. The frequency diverse array (FDA), which uses a tiny frequency offset among antenna elements, has recently applied to the transmitting array elements of MIMO radar to offer the capability of a range-angle-dependent beampattern and a range-dependent interference suppression [1]-[4]. Specifically, the problem of angle and range estimation for FDA-MIMO radar has drawn much attention for target localization. In [5], the two-dimensional (2D) multiple signal classification (MUSIC), one of the most widely used subspace-based methods, has been used for angle and range estimation and achieves moderate estimation performance. However, such subspace-based methods cannot work under a single measurement condition. In [6], the sparse signal reconstruction method has been explored for angle and range estimation, however, such methods like the orthogonal matching pursuit (OMP) [7] and least absolute shrinkage and selection operator (LASSO) [8] etc., are always subject to the grid-mismatch effect [9], deteriorating the estimation performance.

Recently, gridless atomic norm minimization (ANM) methods for one-dimensional (1D) line spectrum estimation have been derived in [10]-[11]. In [12], a gridless compressive beamforming method based on 2D-ANM for acoustic sources has been proposed. More recently, a low-complexity optimization method named decoupled ANM (DANM) has been explored for 2D direction-of-arrival (DOA) estimation in [13].

In this paper, inspired by [13], a gridless angle and range estimation approach is proposed for FDA-MIMO radar based on DANM. First, the angle and range estimation based on 2D-ANM is converted into a decoupled semi-definite programming (SDP) problem by substituting the original 2D estimation problem with two decoupled 1D Toeplitz Hermitian matrices. Then the matrix enhancement and matrix pencil (MEMP) method [14] is applied and a permutation matrix is constructed to obtain the joint angle and range estimation and parameter pairing. Unlike the subspace-based methods such as 2D-MUSIC, the proposed approach for FDA-MIMO radar can work with a single measurement. Also, it has no grid-mismatch effect of the sparse signal reconstruction-based algorithms such as OMP and LASSO. In addition, compared with the method in [13], in which two enhanced matrices are constructed and the singular value decomposition (SVD) is used twice, in the proposed approach, only one enhanced matrix is constructed, and the SVD is used once.

Notations: We use lower-case (upper-case) bold characters to denote vectors (matrices). In particular, $\mathbf{I}_N$ denotes the $N \times N$ identity matrix. $(\cdot)^*$, $(\cdot)^T$, $(\cdot)^H$ and $(\cdot)^{-1}$ imply conjugate, transpose, conjugate transpose and inverse of matrix, respectively. $\otimes$ denotes the Kronecker product. $\mathrm{diag}(\mathbf{x})$ is a diagonal matrix with vector $\mathbf{x}$ being its diagonal. $\mathrm{eig}(\cdot)$ represents extracting the eigenvalue of a matrix. $\mathrm{angle}(\cdot)$ returns the phase angles, in radians.

The research is supported by the National Natural Science Foundation of China (Nos. 61371158 and 61771217), and Jilin Provincial Natural Science Foundation of China (No.20180101329JC). The corresponding author is Hong Jiang. E-mail: jiangh@jlu.edu.cn

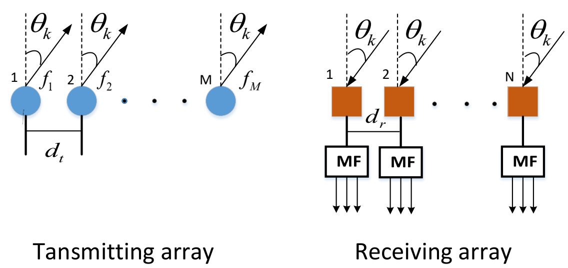

Fig. 1. Configuration of FDA-MIMO radar, "MF" denotes the matched filter

2. SIGNAL MODEL

Assume that a colocated FDA-MIMO radar consists of M uniform linear transmitting elements with element spacing d_t and N uniform linear receiving elements with element spacing d_r. The targets located at far field can be seen at the same direction for all the array elements. Fig.1 shows the configuration of FDA-MIMO radar.

The radiated signal frequency from the m-th transmitting element can be denoted as

$$f_m = f_0 + m\Delta f, \;\; m = 0, 1, \cdots, M-1 \tag{1}$$

where f_0 is the carrier frequency and Δf is the frequency increment, $\Delta f \ll f_0$. The element interval is usually determined as the half wavelength of the maximum transmit frequency to avoid aliasing effects, i.e. $d_t = d_r = c_0/2(f_0 + (M-1)\Delta f)$, where c_0 is the speed of light. The signal emitted from the m-th transmitting array element at time t can be expressed as

$$s_m(t) = \phi_m(t)e^{j2\pi f_m t} \tag{2}$$

where $\phi_m(t)$ is the signal envelope. The transmitting waveforms $s_m(t), m = 1, 2, \cdots, M$ are supposed to be orthogonal to each other.

Consider a far-field scenario and take the first elements of the transmitting and receiving arrays as the reference elements, respectively. Then, for the k-th point target localized at angle θ_k and range r_k, the signal propagation time from the m-th transmitting element to the n-th receiving element can be denoted as

$$\tau(m,n,\theta_k,r_k) = \frac{2r_k}{c_0} - \frac{d_t(m-1)\sin(\theta_k)}{c_0} - \frac{d_r(n-1)\sin(\theta_k)}{c_0} \tag{3}$$

where the first term is a common time delay. The second and third terms are caused by the transmitting and receiving array manifolds, respectively.

Assume that the number of targets is known and there are K targets impinging on the receiving arrays, then the output data of matched filter in the n-th receiving element for the m-th transmitting element is

$$x_{m,n} = \sum_{k=1}^{K} \phi_m(t - \tau(m,n,\theta_k,r_k))e^{j2\pi f_m(t-\tau(m,n,\theta_k,r_k))} \tag{4}$$

After approximation and recombination of output data, the signal model of FDA-MIMO radar can be formulated as

$$\begin{aligned}\mathbf{X} &= \sum_{k=1}^{K} \xi_k \mathbf{a}_r(\psi_k)\mathbf{a}_t(\eta_k)^T + \mathbf{N} \\ &= \mathbf{A}_r(\boldsymbol{\psi})\text{diag}(\boldsymbol{\xi})\mathbf{A}_t(\boldsymbol{\eta})^T + \mathbf{N}\end{aligned} \tag{5}$$

where $\mathbf{X} \in \mathbb{C}^{N\times M}$, $\mathbf{A}_r(\boldsymbol{\psi}) = [\mathbf{a}_r(\psi_1), \mathbf{a}_r(\psi_2), \cdots, \mathbf{a}_r(\psi_K)] \in \mathbb{C}^{N\times K}$, $\mathbf{a}_r(\psi_k) = [1, e^{j2\pi\psi_k}, \cdots, e^{j2\pi(N-1)\psi_k}]^T$, $\psi_k = \frac{d_r\sin(\theta_k)}{\lambda_0}$, $\lambda_0 = \frac{c_0}{f_0}$, and $\boldsymbol{\xi} = [\xi_1, \xi_2, \cdots, \xi_K]^T$ consists of the phases and amplitudes of the K targets. $\mathbf{A}_t(\boldsymbol{\eta}) = [\mathbf{a}_t(\eta_1), \mathbf{a}_t(\eta_2), \cdots, \mathbf{a}_t(\eta_K)] \in \mathbb{C}^{M\times K}$, where $\mathbf{a}_t(\eta_k) = [1, e^{j2\pi\eta_k}, \cdots, e^{j2\pi(M-1)\eta_k}]^T$, $\eta_k = \frac{d_t\sin(\theta_k)}{\lambda_0} - \frac{\Delta f}{c_0}2r_k$, $\mathbf{N} \in \mathbb{C}^{N\times M}$ is assumed to be independent and zero-mean complex Gaussian noise. From (5), we see that $\mathbf{A}_t(\boldsymbol{\eta})$ consists (θ_k, r_k) and $\mathbf{A}_r(\boldsymbol{\psi})$ consists θ_k for $k = 1, \cdots, K$. Our goal is to estimate (θ_k, r_k) from the observed matrix $\mathbf{X}$.

3. ANGLE AND RANGE ESTIMATION WITH DANM

3.1. Atomic Norm

Let us review the concept of atomic norm [15]. Let $\mathcal{A}$ be a collection of atoms satisfying that its convex hull, conv($\mathcal{A}$), is compact and centrally symmetric. Then the atomic norm induced by conv($\mathcal{A}$) is

$$\|\mathbf{y}\|_{\mathcal{A}} \triangleq \{t|\mathbf{y} \in t\text{conv}(\mathcal{A}), t \geq 0\} \tag{6}$$

The norm $\|\mathbf{y}\|_{\mathcal{A}}$ is only evaluated for those $\mathbf{y}$ that lie in the affine hull of conv($\mathcal{A}$).

3.2. Matrix-Form Atomic Norm and DANM

According to [13] and (6), the matrix-form atom set $\mathcal{A}$ is defined as

$$\mathcal{A} \triangleq \{\mathbf{a}_r(\psi)\mathbf{a}_t(\eta)^T, \forall\, \psi \in [-1/2, 1/2], \eta \in [-1/2, 1/2]\} \tag{7}$$

where ψ and η are confined to $[-1/2, 1/2]$ to avoid the phase ambiguity. For ease of presentation, we will ignore the noise temporarily. Then the matrix-form atomic norm of $\mathbf{X}$ with set $\mathcal{A}$ can be denoted as

$$\|\mathbf{X}\|_{\mathcal{A}} = \left\{\sum_k |h_k| \;\middle|\; \sum_k h_k \mathbf{a}_r(\psi_k)\mathbf{a}_t(\eta_k)^T, \mathbf{a}_r(\psi_k)\mathbf{a}_t(\eta_k)^T \in \mathcal{A}\right\} \tag{8}$$

To obtain the angle and range estimation, the next step is to obtain the minimization of $\|\mathbf{X}\|_{\mathcal{A}}$. When the observation $\mathbf{X}$ is contaminated with noise, the de-noising formulation is

$$\min_{\mathbf{X}_v} \|\mathbf{X}_v\|_{\mathcal{A}} + \zeta \|\mathbf{X} - \mathbf{X}_v\|_2^2 \tag{9}$$

where $\mathbf{X}_v$ is regarded as the noise-free observation and the regularization parameter ζ can be referenced in [16] for details. Then (9) can be converted to a decoupled SDP problem

$$\begin{aligned} \min_{\mathbf{X}_v, \boldsymbol{w}_1, \boldsymbol{w}_2} & \frac{1}{2\sqrt{MN}}(\mathbf{T}(\boldsymbol{w}_1) + \mathbf{T}(\boldsymbol{w}_2)) + \zeta \|\mathbf{X} - \mathbf{X}_v\|_2^2 \\ s.t. \quad & \begin{bmatrix} \mathbf{T}(\boldsymbol{w}_1) & \mathbf{X}_v \\ \mathbf{X}_v^H & \mathbf{T}(\boldsymbol{w}_2) \end{bmatrix} \geq 0 \end{aligned} \tag{10}$$

where $\mathbf{T}(\boldsymbol{w}_1) \in \mathbb{C}^{N\times N}$ and $\mathbf{T}(\boldsymbol{w}_2) \in \mathbb{C}^{M\times M}$ are one-level Hermitian Toeplitz matrices defined by the first rows $\boldsymbol{w}_1 \in \mathbb{C}^N$ and $\boldsymbol{w}_2 \in \mathbb{C}^M$, respectively. Then (10) can be solved by off-the-shelf solvers such as SDPT3 [17]. The optimal solution $\mathbf{T}(\tilde{\boldsymbol{w}}_1)$, $\mathbf{T}(\tilde{\boldsymbol{w}}_2)$ and $\tilde{\mathbf{X}}_v$ are denoted as $\mathbf{T}(\tilde{\boldsymbol{w}}_1) = \mathbf{A}_r(\tilde{\boldsymbol{\psi}})\text{diag}(\tilde{\mathbf{h}})\mathbf{A}_r(\tilde{\boldsymbol{\psi}})^H$, $\mathbf{T}(\tilde{\boldsymbol{w}}_2) = \mathbf{A}_t(\tilde{\boldsymbol{\eta}})^*\text{diag}(\tilde{\mathbf{h}})\mathbf{A}_t(\tilde{\boldsymbol{\eta}})^T$ and $\tilde{\mathbf{X}}_v = \mathbf{A}_r(\tilde{\boldsymbol{\psi}})\text{diag}(\tilde{\mathbf{h}})\mathbf{A}_t(\tilde{\boldsymbol{\eta}})^T$, respectively.

3.3. MEMP Method for Angle and Range Estimation

In this section, we apply the MEMP method to $\tilde{\mathbf{X}}_v$ to obtain the two estimates $\tilde{\boldsymbol{\psi}}$ and $\tilde{\boldsymbol{\eta}}$. An enhanced matrix is defined through a partition-and-stacking process as follows:

$$\mathbf{Y} = \begin{bmatrix} \mathbf{Y}_1 & \mathbf{Y}_2 & \cdots & \mathbf{Y}_{N+1-P} \\ \mathbf{Y}_2 & \mathbf{Y}_3 & \cdots & \mathbf{Y}_{N+2-P} \\ \vdots & \vdots & \ddots & \vdots \\ \mathbf{Y}_P & \mathbf{Y}_{P+1} & \cdots & \mathbf{Y}_N \end{bmatrix} \tag{11}$$

where

$$\mathbf{Y}_i = \begin{bmatrix} \tilde{\mathbf{X}}_v(i,1) & \tilde{\mathbf{X}}_v(i,2) & \cdots & \tilde{\mathbf{X}}_v(i,M+1-Q) \\ \tilde{\mathbf{X}}_v(i,2) & \tilde{\mathbf{X}}_v(i,3) & \cdots & \tilde{\mathbf{X}}_v(i,M+2-Q) \\ \vdots & \vdots & \ddots & \vdots \\ \tilde{\mathbf{X}}_v(i,Q) & \tilde{\mathbf{X}}_v(i,Q+1) & \cdots & \tilde{\mathbf{X}}_v(i,M) \end{bmatrix} \tag{12}$$

where $\tilde{\mathbf{X}}_v(i,j)$ ($i = 1,2,\cdots,N$, $j = 1,2,\cdots,M$) is the (i,j) element of $\tilde{\mathbf{X}}_v$. P and Q is always assumed to be $\frac{N+1}{2}$ and $\frac{M+1}{2}$, as long as the computational burden is tolerable [14].

Then applying the SVD to $\mathbf{Y}$, we can obtain

$$\mathbf{Y} = \mathbf{U}\boldsymbol{\Lambda}\mathbf{V}^H = \mathbf{U}_s\boldsymbol{\Lambda}_s\mathbf{V}_s^H + \mathbf{U}_n\boldsymbol{\Lambda}_n\mathbf{V}_n^H \tag{13}$$

where $\mathbf{U}$ and $\mathbf{V}$ are unitary matrices whose columns are the left and right singular vectors. $\boldsymbol{\Lambda}$ contains a diagonal matrix with the singular values in the descending order. The subindexes s and n stand for the subspaces of signal and noise, respectively.

Construct $\mathbf{U}_1$ which is $\mathbf{U}_s$ with the last Q rows deleted, and $\mathbf{U}_2$ which is $\mathbf{U}_s$ with the first Q rows deleted.

The estimate of $\boldsymbol{\psi}$ is

$$\tilde{\boldsymbol{\psi}} = \frac{\text{angle}(\text{eig}((\mathbf{U}_1^H\mathbf{U}_1)^{-1}\mathbf{U}_1^H\mathbf{U}_2))}{2\pi} \tag{14}$$

Next, construct a permutation matrix

$$\boldsymbol{\Gamma} = \begin{bmatrix} \mathbf{e}(1) \\ \mathbf{e}(1+Q) \\ \cdots \\ \mathbf{e}(1+(P-1)Q) \\ \mathbf{e}(2) \\ \mathbf{e}(2+Q) \\ \cdots \\ \mathbf{e}(2+(P-1)Q) \\ \cdots \\ \cdots \\ \mathbf{e}(Q) \\ \mathbf{e}(Q+Q) \\ \cdots \\ \mathbf{e}(Q+(P-1)Q) \end{bmatrix} \tag{15}$$

where $\mathbf{e}(i)$ is a $1 \times PQ$ vector with one at the i-th position and zero everywhere else.

Construct $\mathbf{U}_3$ which is $\boldsymbol{\Gamma}\mathbf{U}_s$ with the last P rows deleted, and $\mathbf{U}_4$ which is $\boldsymbol{\Gamma}\mathbf{U}_s$ with the first P rows deleted.

The estimate of $\boldsymbol{\eta}$ is

$$\tilde{\boldsymbol{\eta}} = \frac{\text{angle}(\text{eig}((\mathbf{U}_3^H\mathbf{U}_3)^{-1}\mathbf{U}_3^H\mathbf{U}_4))}{2\pi} \tag{16}$$

3.4. Angle and Range Estimation Pairing

The pairing function can be denoted as

$$\begin{aligned} f(k) = \arg\max_{i\in\{1,2,\cdots,K\}} & \Big\|\mathbf{U}_s^H([1, e^{j2\pi\tilde{\eta}_i}, \cdots, e^{j2\pi\tilde{\eta}_i(P-1)}]^T \\ & \otimes[1, e^{j2\pi\tilde{\psi}_k}, \cdots, e^{j2\pi\tilde{\psi}_k(Q-1)}]^T)\Big\|_2 \end{aligned} \tag{17}$$

where $k = 1,2,\cdots,K$. Then for each $\tilde{\psi}_k$, the parameter $\tilde{\eta}_{f(k)}$ can be paired with it. For the k-th target, the estimate of angle is $\tilde{\theta}_k = \arcsin(\frac{\tilde{\psi}_k\lambda_0}{d_r})$, and the estimate of range is $\tilde{r}_{f(k)} = \frac{\tilde{\psi}_k d_t c_0}{2d_r\Delta f} - \frac{c_0\eta_{f(k)}}{2\Delta f}$.

3.5. Resolution of ANM

Using convex optimization methods to (10) is the necessity of a particular resolution condition. The minimum resolvable $\Delta_{\psi,min}$ and $\Delta_{\eta,min}$ should be more than $\frac{4}{N}$ and $\frac{4}{M}$, theoretically. However, in actual situations, it is enough only if $\Delta_{\psi,min}$ and $\Delta_{\eta,min}$ are more than $\frac{1}{N}$ and $\frac{1}{M}$ (maybe even less) [10], respectively. In addition, the number of targets should be no more than $\min\{M,N\}$.

4. NUMERICAL EXAMPLES

In this section, numerical examples are conducted to validate the performance of the proposed method.

4.1. Experiment 1

Consider a colocated FDA-MIMO radar with 10 transmitting elements and 10 receiving elements. The carrier frequency is $f_0 = 10\,GHz$, and the linear frequency increment is $\Delta f = 5\,KHz$. Assume that there are two targets with $[\theta, r] = [(0°, 11\,km), (15°, 4\,km)]$. A single measurement is assumed. We compare the proposed approach with the subspace-based MUSIC method [5] and the sparse reconstruction-based OMP algorithm [7] for angle and range estimation. For the OMP algorithm, the uniform searching dictionaries of angle and range are $[-20°, -20° + \delta_a, \cdots, 40° - \delta_a, 40°]$ and $[0, \delta_r, \cdots, 14 - \delta_r, 14]\,km$, respectively. Assume that there are two different element intervals of searching dictionaries: $t1$ is $[\delta_a, \delta_r] = [0.5°, 0.1km]$ and $t2$ is $[\delta_a, \delta_r] = [1.5°, 0.3km]$. We observe that the real angles and ranges of the two targets lie in the $t1$ dictionary but not in the $t2$ dictionary. The performance of root mean square error (RMSE) is examined with 100 Monte Carlo (MC) trials. The results are shown in Fig. 2.

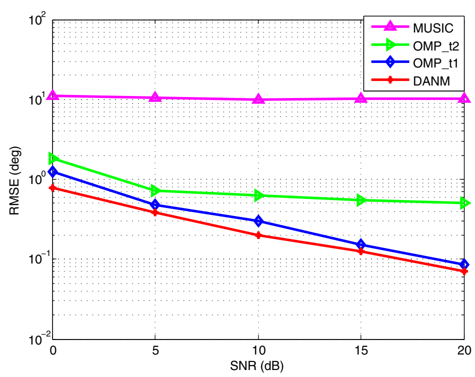

(a) RMSE versus SNR for angle estimation

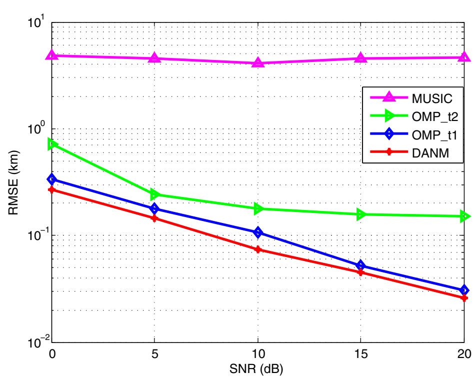

(b) RMSE versus SNR for range estimation

Fig. 2. RMSE performance

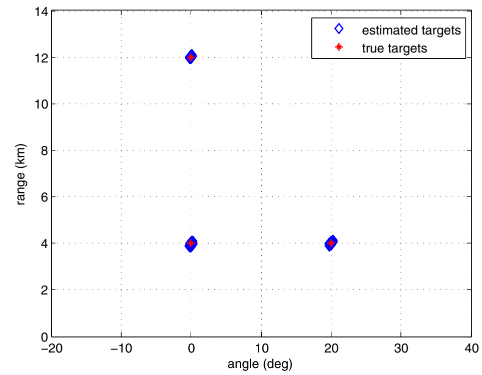

Fig. 3. Angle-range estimation result of the proposed method

From Fig.2 we can see that the MUSIC method has lost the estimation efficiency due to the rank deficiency of covariance matrix with only one measurement. As for the OMP method, since the real angles and ranges of the two targets do not lie in the $t2$ dictionary, the estimation accuracy of the OMP-$t2$ method deteriorates seriously compared with that of the OMP-$t1$ method, leading to the grid-mismatch effect. Although the real angles and ranges lie in the $t1$ dictionary, the OMP-$t1$ method still has lower estimation accuracy compared with the proposed DANM-based approach. Therefore, the proposed approach overcomes the defects of the MUSIC and OMP methods and achieves the highest accuracy.

4.2. Experiment 2

In this experiment, consider a colocated FDA-MIMO radar with 12 transmitting elements and 12 receiving elements. Assume that $SNR = 15dB$ and there are three targets with $[\theta, r] = [(0°, 4\,km), (0°, 12\,km), (20°, 4\,km)]$. We observe that the target 1 and target 2 own the identical angle, and the target 1 and target 3 own the identical range. Other simulation conditions are the same with Experiment 1. We make 100 MC trials. Fig.3 shows the estimation result of the proposed DANM-based method. From Fig.3 we see that regardless of whether the targets are at the same angle with different ranges, or at the same range with different angles, the proposed approach performs well with a single measurement.

5. CONCLUSION

In this paper, we investigate the signal model of FDA-MIMO radar and explore the problem of joint angle and range estimation. A novel gridless parameter estimation approach based on DANM is proposed for FDA-MIMO radar. The proposed approach works well with a single measurement. Compared with conventional sparse reconstruction methods, it is not subject to the grid-mismatch effect. In addition, the estimated parameters can pair each other well. Therefore, it is suitable for many actual applications of FDA-MIMO radar.

6. REFERENCES

[1] P. Antonik, M. C. Wicks, H. D. Griffiths and C. J. Baker, “Frequency diverse array radars,” 2006 IEEE Conference on Radar, Verona, NY, USA

[2] W. Wang and H. C. So, “Transmit Subaperturing for Range and Angle Estimation in Frequency Diverse Array Radar,” IEEE Transactions on Signal Processing, vol. 62, no. 8, pp. 2000-2011, April 15, 2014.

[3] J. Xu, G. Liao, S. Zhu, L. Huang and H. C. So, “Joint Range and Angle Estimation Using MIMO Radar With Frequency Diverse Array,” IEEE Transactions on Signal Processing, vol. 63, no. 13, pp. 3396-3410, July 1, 2015.

[4] S. Brady, “Frequency diverse array radar: signal characterization and measure-ment accuracy,” Master’s thesis, Air Force Institute of Technology, 2010.

[5] J. Xiong, W. Wang and K. Gao, “FDA-MIMO Radar Range-Angle Estimation: CRLB, MSE, and Resolution Analysis,” IEEE Transactions on Aerospace and Electronic Systems, vol. 54, no. 1, pp. 284-294, Feb. 2018.

[6] H. Chen and H. Shao, “Sparse reconstruction based target localization with frequency diverse array MIMO radar,” 2015 IEEE China Summit and International Conference on Signal and Information Processing (ChinaSIP), Chengdu, 2015, pp. 94-98.

[7] J. A. Tropp and A. C. Gilbert, “Signal Recovery From Random Measurements Via Orthogonal Matching Pursuit,” IEEE Transactions on Information Theory, vol. 53, no. 12, pp. 4655-4666, Dec. 2007.

[8] Tibshirani, Robert. 1996. “Regression Shrinkage and Selection via the lasso,” Journal of the Royal Statistical Society. Series B (methodological) 58 (1). Wiley: 267-288.

[9] Y. Chi, L. L. Scharf, A. Pezeshki and A. R. Calderbank, “Sensitivity to Basis Mismatch in Compressed Sensing,” IEEE Transactions on Signal Processing, vol. 59, no. 5, pp. 2182-2195, May 2011.

[10] G. Tang, B. N. Bhaskar, P. Shah and B. Recht, “Compressed Sensing Off the Grid,” IEEE Transactions on Information Theory, vol. 59, no. 11, pp. 7465-7490, Nov. 2013.

[11] Z. Yang and L. Xie, “On Gridless Sparse Methods for Line Spectral Estimation From Complete and Incomplete Data,” in IEEE Transactions on Signal Processing, vol. 63, no. 12, pp. 3139-3153, June15, 2015.

[12] Y. Yang, Z. Chu, Z. Xu and G. Ping, “Two-dimensional grid-free compressive beamforming,” The Journal of the Acoustical Society of America, vol.142, no. 2, pp. 618-629, 2017

[13] Z. Tian, Z. Zhang and Y. Wang, “Low-complexity optimization for two-dimensional direction-of-arrival estimation via decoupled atomic norm minimization,” 2017 IEEE International Conference on Acoustics, Speech and Signal Processing (ICASSP), New Orleans, LA, 2017, pp. 3071-3075.

[14] Y. Hua, “Estimating two-dimensional frequencies by matrix enhancement and matrix pencil,” IEEE Transactions on Signal Processing, vol. 40, no. 9, pp. 2267-2280, Sept. 1992.

[15] J. Giménez, R. Botella-Estrada, D. Hemández, “The Convex Geometry of Linear Inverse Problems,” Foundations of Computational Mathematics, vol. 12, no. 6, pp. 805-849, 2012

[16] B. N. Bhaskar, G. Tang, and B. Recht, “Atomic norm denoising with applications to line spectral estimation,” IEEE Transactions on Signal Processing, vol. 61, no. 23, pp. 5987-5999, Dec. 2013.

[17] K. C. Toh, R. H. Tutuncu and M. J. Todd, “On the implementation of SDPT3 (version 3.1) - a MATLAB software package for semidefinite-quadratic-linear programming,” 2004 IEEE International Conference on Robotics and Automation (IEEE Cat. No. 04CH37508), New Orleans, LA, 2004, pp. 290-296.